EXPANDING THE CAPABILITIES OF CHILI WITH FEMTOSECOND LASER ABLATION. A. Regula[1,2], T. Stephan[1,2], J. M. Korsmeyer[2,3], A. M. Davis[1,2,4], and N. Dauphas[1,2,4], [1]Department of the Geophysical Sciences, The University of Chicago, Chicago, IL, USA, [2]Chicago Center for Cosmochemistry, [3]Department of Chemistry, The University of Chicago, Chicago, IL, USA, [4]Enrico Fermi Institute, The University of Chicago, Chicago, IL, USA. (regula@uchicago.edu)

Introduction: The Chicago Instrument for Laser Ionization (CHILI) was designed to measure the isotopic compositions of small samples at high spatial resolution and high sensitivity [1]. Resonance ionization, by which CHILI ionizes neutral atoms, offers the potential for analysis of elements at trace concentrations, with high useful yield, and without the same potential for isobaric interferences as secondary ion mass spectrometry (SIMS) and laser ablation inductively coupled plasma mass spectrometry (LA-ICPMS). To generate neutral atoms for ionization, an Orsay Physics Cobra Ga^+ ion gun and an Photonics Industries DC150 351 nm Nd:YLF desorption laser with a pulse length of ~24 ns were included in CHILI's original design [1]. As ion beam intensities are rather limited, the ion gun is mainly useful for analyzing elements at high concentrations. However, when analyzing materials with elements at lower concentrations, the desorption laser is required. An ablation laser is capable of depositing far more energy per pulse than the Ga ion gun, allowing ablation of more material on shorter time scales. The original desorption laser has been used to successfully analyze, e.g., presolar SiC and graphite grains [e.g., 2–5], chondrules [6], apatite inclusions in zircon [7], and metals [8]. However, analyses of many minerals, including hibonite [9], and glasses have not been possible due to transparency of these materials to 351 nm laser light.

To broaden the range of materials accessible to CHILI, including the aforementioned transparent materials, a Light Conversions Pharos femtosecond ablation laser was acquired and recently installed. Here, we report first results obtained with the new laser operating with a wavelength of 343 nm and a pulse length of 190 fs by analyzing Mo and Ba in NIST SRM 610 glass [10, 11] and Mo and Ru in the type IVB iron meteorite Santa Clara, which had been analyzed before with the original setup [12].

Materials: CHILI works via RIMS (resonance ionization mass spectrometry), where neutral atoms (as well as molecules and secondary monatomic and molecular ions) are desorbed from a target surface, and the atoms of two or three target chemical elements are ionized by lasers tuned to element-specific wavelengths targeting electronic transitions. For this work, the instrument was set up to measure Ru, Mo, and Ba.

Our Pharos laser from Light Conversion is capable of producing wavelengths of 1030, 515, and 343 nm. At 1030 nm the pulse length is adjustable from ~180 fs to 10 ps. At 515 and 343 nm, the pulse length is fixed at ~180 fs. The beam is focused onto the sample using the same Schwarzschild microscope and transport optics as used for the original desorption laser [1], therefore we are currently running the Pharos at 343 nm wavelength.

Femtosecond laser ablation is a process by which bonds in the sample are broken by highly energetic and very short-duration pulses of laser energy. This is a non-thermal process, as energy delivery and bond-breaking occur on a shorter timescale than that of the transfer of delivered energy from the electrons into the lattice of the sample material [13]. No melting occurs in the sample, and so there should be minimal chance for thermal fractionation of desorbed material. This is one of the main differences compared to laser desorption at nanosecond pulse lengths, which typically results in melting and evaporation of the material. Unlike the original laser, to which many silicate minerals and glasses are transparent, and to which no energy can be delivered, femtosecond laser ablation will work irrespective of sample composition. Multi-photon absorption and tunnel ionization effects induced by femtosecond laser pulsing impart sufficient energy for ablation even in materials transparent to the laser's wavelength [14]. Certain materials create analytical conditions that vary with wavelength of incoming laser light (e.g., nonresonant ionization may be less likely with longer wavelengths), and so the three wavelength outputs of the Pharos will present a range of options to optimize the process for various sample compositions.

Each measurement on the NIST SRM 610 glass or Santa Clara consisted of ~1–5×10^6 shots rastered over a 10×10 μm^2 area, preceded by a pre-sputter over a 20×20 μm^2 area to remove the conductive gold coating from the surface. Measurements were made during the same session with both the original 351 nm laser and the 343 nm beam of the Pharos, alternating between them in sequence. Ru/Mo relative sensitivity factors were determined as described earlier [12].

Since isotopes of Ru and Mo share isobars at 96 u, 98 u, and 100 u, an alternate shot firing scheme during analysis was used. Ionization lasers for Ru+Ba and Mo were fired on alternating shots of the ablation lasers. This scheme reduces the useful yield by 50%, but it allows for the clear separation of Ru and Mo signals.

Results: *NIST SRM 610* contains 417 ppm Mo and 452 ppm Ba [11], and both elements were easily detectable with CHILI using the Pharos femtosecond laser. Laser ablation occurred in a nonthermal way leaving craters that resemble those typical for ion sputtering. However, relative signal intensities for Mo and Ba were found to vary, such that Ba/Mo ratios increased during the course of the measurement. Isotope ratios, on the other hand, did not change during the measurements and were highly reproducible.

The Ru/Mo relative sensitivity factors (RSFs) measured for Santa Clara were almost identical: 0.210±0.011 with the original 351 nm desorption laser and 0.240±0.011 with the new femtosecond laser.

The 351 nm laser induced melting in the meteorites and their gold coating, and generated bursts of signal through time. The femtosecond laser generates pits showing no evidence of melting (Fig. 1), with consistent signal through time.

Discussion: Silicate minerals and glasses were previously inaccessible to CHILI when equipped solely with the 351 nm desorption laser. As demonstrated here, the addition of a femtosecond ablation laser has resulted in the successful measurement of a silicate glass with CHILI. This is a promising first step in expanding the range of sample compositions that can be analyzed with CHILI.

While these results are promising, the issue of inconsistency in the measured RSFs remains. This inconsistency could be the result of a few potential causes and will require further investigation.

Ru/Mo RSFs measured in the iron meteorite using the Pharos femtosecond laser are very reproducible, with a narrower spread than those reported in the past using either the ion gun or the 351 nm Nd:YLF laser.

Moving forward, more testing will be done on a range of material compositions and over a range of operational conditions in order to optimize our analytical methods using the Pharos. The effects of adjusting timing of the ionization laser firing with respect to ablation laser firing, varying the duration of presputtering, adjusting the size of the rastered area, and varying the pulse length and ablation laser wavelength will be explored.

References: [1] Stephan T. et al. (2016) *Int. J. Mass Spectrom., 407,* 1–15. [2] Trappitsch R. (2018) *GCA, 221,* 87–101. [3] Stephan T. et al. (2018) *GCA, 221,* 109–126. [4] Stephan T. et al. (2019) *ApJ, 877,* 101. [5] Bloom H. E. et al. (2022) *LPS, 53,* #2624. [6] Trappitsch R. et al. (2018) *ApJL, 857,* L15. [7] Boehnke P. et al. (2018) *PNAS, 115,* 6353–6356. [8] Korsmeyer J. M. et al. (2022) *LPS, 53,* #2795. [9] Kööp L. et al. (2016) *MAPS, 51,* #6443). [10] Kane J. S. (1998) *Geostand. Newslett., 22,* 7–13. [11] Jochum K. P. et. al. (2011) *Geostand. Newslett., 35,* 397–429. [12] Regula A. et al. (2022) *LPS, 53,* #2877. [13] Tulej M. et al. (2021) *Appl. Sci., 11,* 2562. [14] Balling P. and Schou J. (2013) *Rep. Prog. Phys., 76,* 0336502.

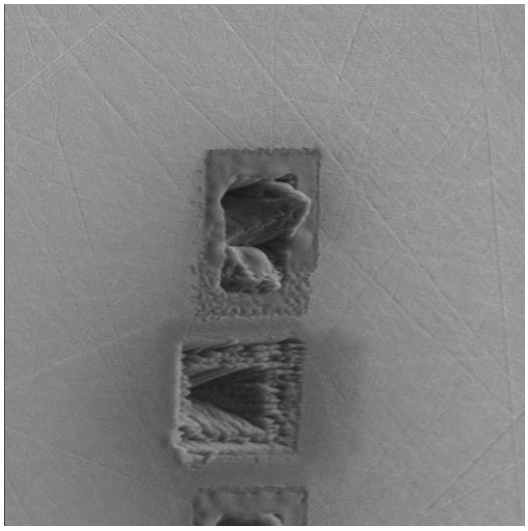

Figure 1: Secondary ion image of laser ablation pits generated with the original laser (top) and Pharos (bottom). Visible are the larger square areas for presputtering (20×20 μm^2) and smaller inner areas (10×10 μm^2) for analysis. Field of view is 100×100 μm^2.